ORIGINAL PAPER

Quantum chemistry investigation on the reaction mechanism of the elemental mercury, chlorine, bromine and ozone system

Zhengyang Gao[1] · Shaokun Lv[1] · Weijie Yang[1] ·
Pengfei Yang[1] · Shuo Ji[1] · Xinxin Meng[1]

Abstract Ab initio calculations were performed to study the quantum chemistry reactions mechanisms among Hg^0, elemental halogen and O_3. The geometry of reactions, transition states (TS), intermediates (M) and products were optimized using the MP2 method at the SDD basis function level for Hg, and using 6-311++G (3df, 3pd) for other species. Molecular energies were calculated at QCISD (T) level with zero point energy. Activation energies were calculated along with pre-exponential factors. The reaction rate constants within 298–1800 K were calculated according to transition state theory (TST). The influences of O_3 on the reaction of Hg^0 with halogen are discussed. Hg^0 can be oxidized to Hg^{1+} by halogen and O_3, and halogen and O_3 can be arranged in decreasing order as: $Br_2 > BrO > O_3 > Br > Cl$, $BrCl > HBr > HCl$, $Br_2 > Cl_2$ according to reaction rate constants. When O_3 is presented, Br_2, HBr, BrCl, Cl_2 and HCl react with O_3 and are initially converted to BrO and ClO. O_3 is unfavorable for oxidation of Hg^0 by Br_2. The mixture of HBr and O_3 has better oxidizing Hg^0 performance than HBr and O_3. Cl is less effective than Br for oxidation of Hg^0.

Keywords Mercury · Quantum chemistry calculation · O_3 · Halogen species · Coal combustion

Introduction

The regulation of mercury emissions from coal-fired boilers is a concern for the electric utility industry. Mercury is of

✉ Shaokun Lv
lskmail@163.com

[1] School of Energy and Power Engineering, North China Electric Power University, Baoding 071003, China

sufficiently high volatility that it will be completely released into flue gas mainly in the form of gas-phase elemental mercury during coal combustion [1, 2]. As the temperature falls during the flow process, the elemental mercury will be oxidized and captured continually by fly ash.

Mercury in flue gas is most commonly classified into three forms: elemental mercury (Hg^0), oxidized mercury (Hg^{2+}) and particulate-bound mercury (Hg_P) [3, 4]. The forms of mercury existing in the flue gas significantly affect the extent to which it is captured in air pollution control devices. Compared to elemental mercury, Hg^{2+} is slightly less volatile at stack temperature and is water-soluble, so it is more readily removed from flue gases in scrubber systems, and has a much shorter atmospheric life time [5–7]. Hg_P can be removed in dust collectors. Several factors are responsible for the conversion of elemental Hg to its oxidized form. The key components in the flue gas are halogen species. Other components such as NO and SO_2 also play important roles [8, 9].

A variety of Hg control technologies have been developed. Sorbents can capture Hg^{2+} effectively, but because of the rather low concentration of Hg in flue gas, the sorbent/Hg ratio has to be high to guarantee a satisfactory Hg removal efficiency, which is very costly. Another approach is to add oxidants such as halogen species into the coal or flue gas to enhance transformation of Hg^0 to Hg^{2+} or Hg_p. Br species can oxidize Hg^0 effectively [10–12]. Niksa [13] described a detailed reaction mechanism for Hg oxidation by Br species in flue gas, which showed that Br species were much more effective than Cl species. O_3 can also oxidize Hg^0 [14], and ionization of O_2 in electrostatic precipitators (ESP) inevitably leads to generation of O_3. However, studies on the reaction mechanisms of O_3 with Br species are scarce, and the influences of O_3 on reactions between Hg^0 and Br species are still unclear.

Owing to the low concentrations of trace element compounds in flue gas and the short duration of transition states
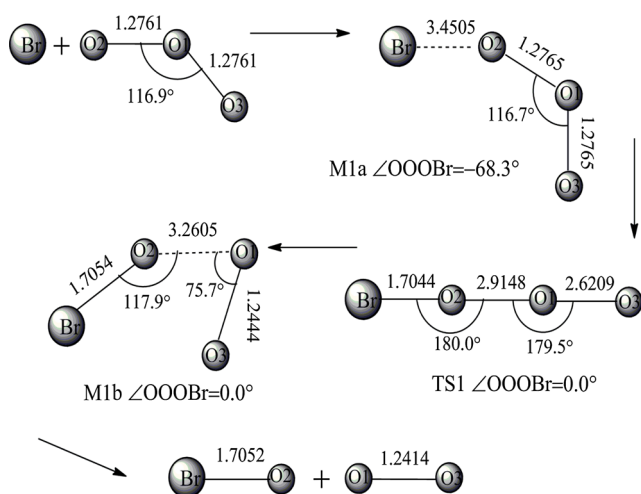
Fig. 1 Reaction process of reaction (*1*): Br+O$_3$→BrO+O$_2$

(TS), it is difficult to find TS structures accurately by experiment [15, 16]. Quantum chemistry calculations are the most accurate theoretical method with which to calculate the structure and energy of the molecular geometry, and can avoid measurement error and artificial estimation [17].

Therefore, quantum chemistry calculations were performed to reveal the reaction mechanisms of the Hg^0-Br-O$_3$ and Hg^0-Cl-O$_3$ systems, and to determine the influences of O$_3$ on Hg^0 oxidation by halogen species.

Computational methodology

The reactions were studied using ab initio calculations of quantum chemistry. The mercury atom has 80 electrons, and a pseudo
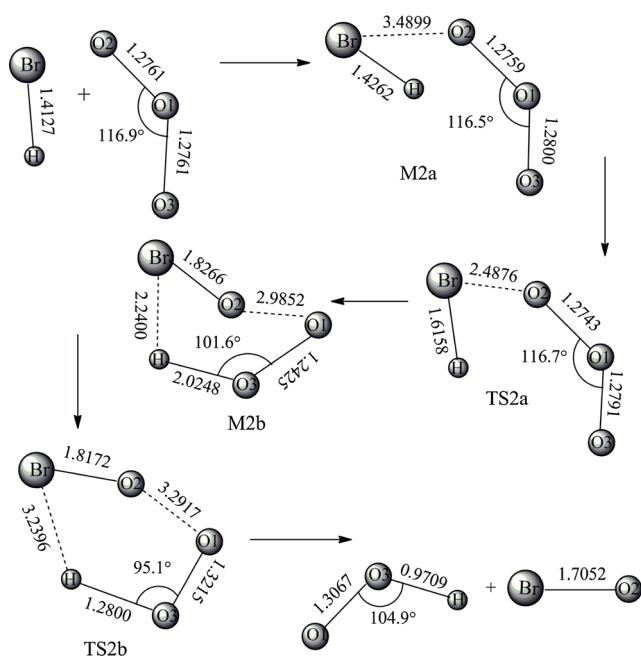

Fig. 3 Reaction process of reaction (*3*): Br$_2$+O$_3$→2BrO+O

potential basis set was used for Hg to guarantee calculation accuracy. Diffuse functions were added for Br, Cl, O and H to increase the extent of valence orbit distribution in space. The geometry configuration of the reactants, products, intermediates (M) and TS were optimized by the MP2 method at the SDD basis function level for Hg, and 6-311++G (3df,3pd) for the other species. Vibration frequency analyses were carried out to ensure that M and TS were reliable. The energies were calculated by the QCISD (T) method with zero point energy (ZPE).

The rate constant k was defined by the rate equation of the classic transition state theory (TST) [18, 19].

$$k = (k_B T/h) \cdot (Q^{\neq}/Q_A Q_B) T^n \cdot \exp(-Ea/RT)$$

where, k_B is the Boltzman constant, T is the thermodynamic temperature, h is Planck's constant, T is the temperature, n is
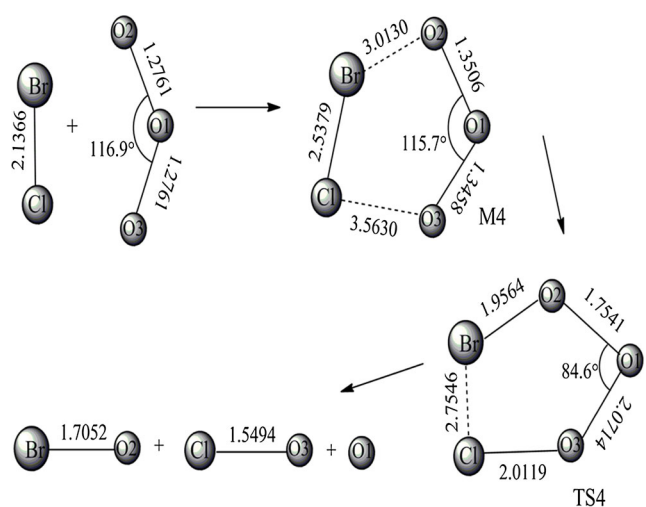

Fig. 2 Reaction process of reaction (*2*): HBr+O$_3$→HgO+O$_2$

Fig. 4 Reaction process of reaction (*4*): BrCl+O$_3$→BrO+ClO+O
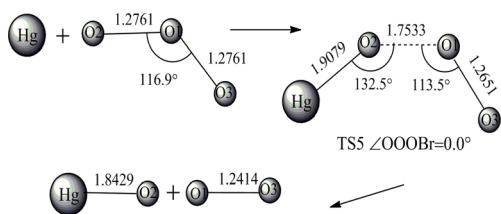
Fig. 5 Reaction process of reaction (5): Hg+O_3→HgO+O_2

the temperature exponent and generally set to zero, Ea is the activation energy, R is the gas constant, $Q^{\neq}$ is the partial function of transition state, and Q_A and Q_B are the partial functions of reactants, respectively.

For Hg^0 oxidation, the conversion of Hg^0 to Hg^{1+} is the dominant step [20–23]. therefore, this paper pays close attention to the influence of O_3 on reactions that convert Hg^0 to Hg^{+1}. Sixteen reactions were calculated: reaction (1)–(4) are the reactions between O_3 and Br species, while reactions (11)–(12) are the reactions between O_3 and Cl species. In Reaction (5), Hg^0 is

oxidized by O_3. Reactions (6)–(10) are the oxidization processes of Hg^0 by Br species. Reactions (13)–(16) are the oxidization processes of Hg^0 by Cl species, and have been studied by other scholars [24, 25] but with different basis sets. In this paper, all of the above reactions were calculated and the kinetic and thermodynamic parameters were obtained using the same basis set.

$$Br + O_3 \rightarrow BrO + O_2 \tag{1}$$

$$HBr + O_3 \rightarrow BrO + HO_2 \tag{2}$$

$$Br_2 + O_3 \rightarrow 2BrO + O \tag{3}$$

$$BrCl + O_3 \rightarrow BrO + ClO + O \tag{4}$$

$$Hg + O_3 \rightarrow HgO + O_2 \tag{5}$$

$$Hg + BrO \rightarrow HgBr + O \tag{6}$$

$$Hg + Br \rightarrow HgBr \tag{7}$$

$$Hg + HBr \rightarrow HgBr + H \tag{8}$$

$$Hg + Br_2 \rightarrow HgBr + Br \tag{9}$$
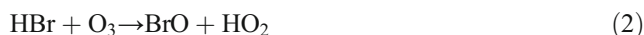
Fig. 6 Reaction process of reaction (11): Cl_2+O_3→2ClO+O

$$Hg + BrCl \rightarrow HgCl + Br \tag{10}$$

$$Cl_2 + O_3 \rightarrow 2ClO + O \tag{11}$$

$$HCl + O_3 \rightarrow ClO + HO_2 \tag{12}$$

$$Hg + HCl \rightarrow HgCl + H \tag{13}$$

$$Hg + Cl \rightarrow HgCl \tag{14}$$

$$Hg + Cl_2 \rightarrow HgCl + Cl \tag{15}$$

$$Hg + Cl_2 \rightarrow HgCl_2 \tag{16}$$
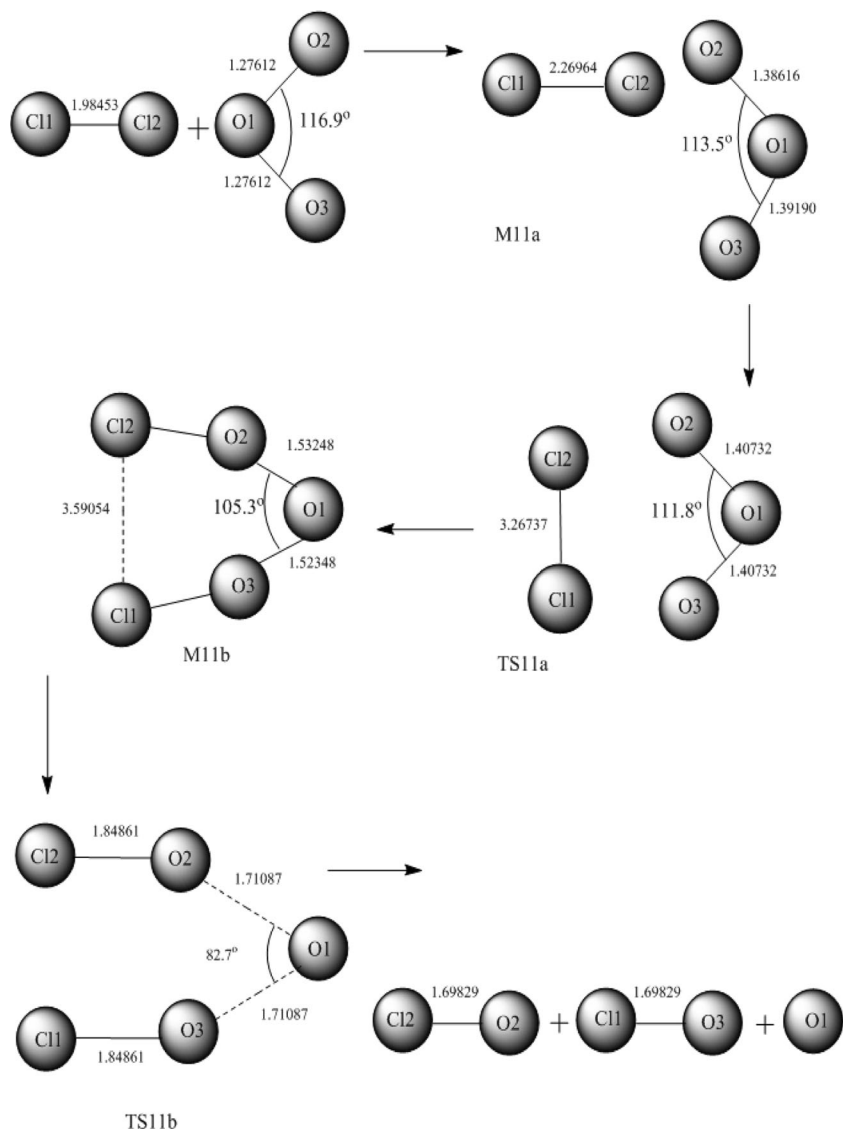
Results and discussion

Mechanism for O_3 reaction with halogen species

The reaction processes are shown in Figs. 1, 2, 3, 4, 5, 6 and 7. In reaction (1), the Br atom reacts with O_3 and M1a forms, then M1a breaks down into BrO and O_2 via TS1 and M1b. During the process, the distance between the Br atom and O

(2) reduces gradually as: 0.3450 nm→0.1704 nm→ 0.1705 nm→0.1705 nm, and the distance between O (2) and O (1) increases gradually as: 0.1276 nm→0.1277 nm→ 0.2915 nm→0.3261 nm.

Reactions (2) and (3) are complicated compared with reaction (1), and have two transition states (TS) and two intermediates (M). For reaction (2), the process is $HBr+O_3 \rightarrow M2a \rightarrow TS2a \rightarrow M2b \rightarrow TS2b \rightarrow BrO+HO_2$. The distance between the Br atom and O (2) reduces gradually as: 0.3490 nm→ 0.2488 nm→0.1827 nm→0.1817 nm→0.1705 nm, the distance between O (2) and O (1) reduces initially, then increases gradually as: 276 nm→0.1275 nm→0.1274 nm→ 0.2985 nm→0.3292 nm. It can be seen from Fig. 3 that the structural transformation in reaction (3) is basically symmetrical. The distances between Br (2) and O (2), Br (1) and O (3) reduce gradually, while the distances between O (2) and O (1), O (1) and O (3) increase gradually.

In reaction (4), BrCl reacts with O_3 forming M4, then M4 breaks down into the products via TS4. During the reaction

Fig. 7 Reaction process of reaction (12): $HCl+O_3 \rightarrow ClO+HO_2$
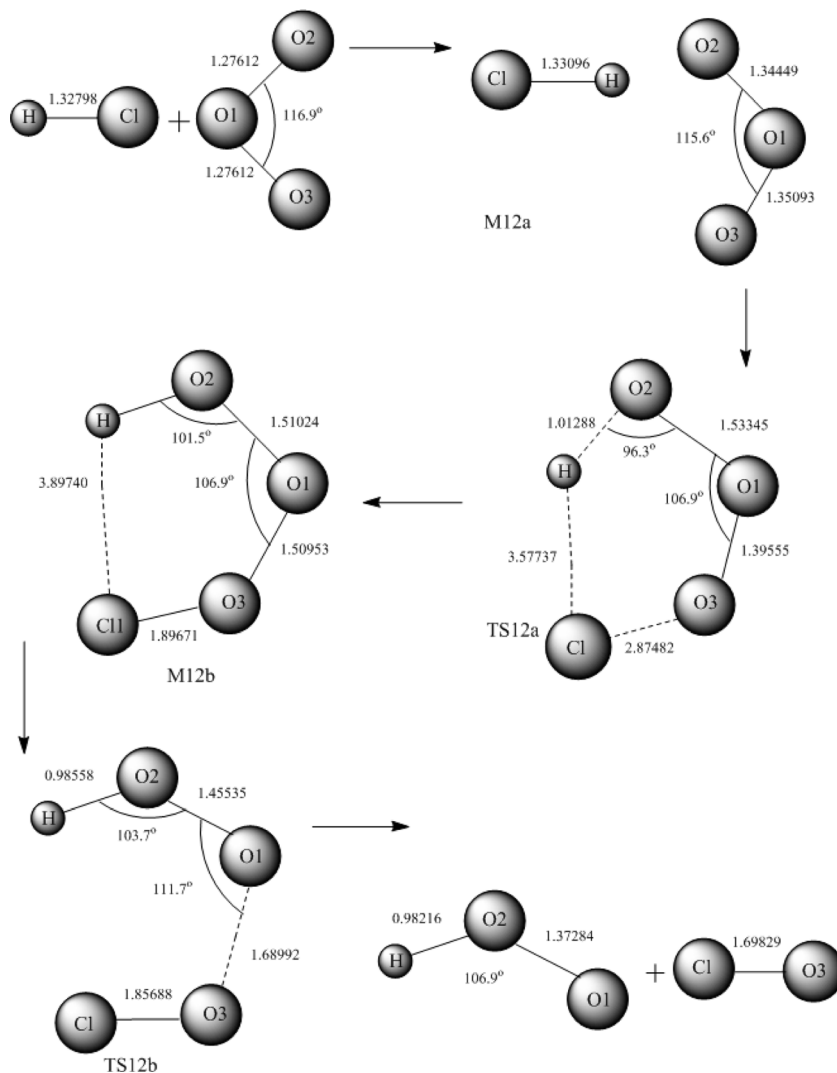
Table 1 The stagnation point energy of each reaction channel (T=298 K). *ZPE* Zero point energy, E_{tot} sum of QCISD (T) energy and ZPE, E_{rel} relative energy

Reaction		MP2 (a.u.)[a]	QCISD (T) (a.u.)	ZPE (a.u.)	E_{tot} (a.u.)	E_{rel} (kcal mol^{-1})
(1)	$Br+O_3$	−2797.610908	−2797.600825	0.00943	−2797.591339	0
	M1a	−2797.613186	−2797.602038	0.00562	−2797.596418	−3.19
	TS1	−2797.432146	−2797.513832	0.00218	−2797.511652	50.00
	M1b	−2797.635126	−2797.669371	0.02031	−2797.649061	−36.22
	$BrO+O_2$	−2797.587721	−2797.587575	0.00464	−2797.58294	5.27
(2)	$HBr+O_3$	−2797.556896	2797.543968	0.01566	−2797.528310	0
	M2a	−2797.675888	−2797.657773	0.01651	−2797.641268	−70.88
	TS2a	−2797.677700	−2797.659787	0.01649	−2797.643302	−72.16
	M2b	−2797.705593	−2797.704981	0.01660	−2797.688382	−100.45
	TS2b	−2797.656490	−2797.654980	0.00896	−2797.646025	−73.87
	$BrO+HO_2$	−2797.686516	−2797.664537	0.01626	−2797.648290	−75.29
(3)	Br_2+O_3	−5369.452883	−5369.440795	0.01021	−5369.430587	0
	M3a	−5369.467901	−5369.451358	0.01233	−5369.439024	−5.30
	TS3a	−5369.465761	−5369.447908	0.01201	−5369.435898	−3.33
	M3b	−5369.475671	−5379.460761	0.01130	−5369.449465	−11.84
	TS3b	−5369.424570	−5369.419877	0.02564	−5369.394236	22.81
	$2BrO+O$	−5369.405372	−5369.398874	0.00333	−5369.395548	21.99
(4)	$BrCl+O_3$	−3256.580933	−3256.572456	0.01048	−3256.561981	0
	M4	−3256.618280	−3256.602573	0.01268	−3256.589893	−17.52
	TS4	−3256.520999	−3256.516077	0.00449	−3256.511592	31.62
	$BrO+ClO+O$	−3256.553261	−3256.534992	0.00322	−3256.531777	18.95
(5)	$Hg+O_3$	−377.756894	−377.784430	0.00943	−377.775000	0
	TS5	−377.708168	−377.731764	0.00580	−377.725964	30.77
	$HgO+O_2$	−377.723542	−377.760140	0.00475	−377.755390	12.31
(6)	$Hg+BrO$	−2800.388659	−2800.417001	0.00166	−2800.415341	0
	TS6	−2800.339911	−2800.379211	0.00101	−2800.378201	23.31
	$HgBr+O$	−2800.395130	−2800.439280	0.00046	−2800.43882	−14.73
(7)	$Hg+Br$	−2725.379110	−2725.40655	0.00000	−2725.406550	0
	TS7	−2725.320370	−2725.344400	0.00000	−2725.344400	39.00
	HgBr	−2725.398112	−2725.419950	0.00046	−2725.419480	−8.11
(8)	$Hg+HBr$	−2725.99899	−2726.015573	0.00623	−2726.009343	0
	TS8	−2725.85379	−2725.879335	0.00071	−2725.878625	82.03
	$HgBr+H$	−2725.88993	−2725.897224	0.00046	−2725.896764	70.64
(9)	$Hg+Br_2$	−5298.100452	−5298.101668	0.00078	−5298.100888	0
	M9	−5298.106952	−5298.115636	0.00090	−5298.114736	−8.69
	TS9	−5298.066703	−5298.08769	0.00084	−5298.086850	8.81
	$HgBr+Br$	−5298.10537	−5298.126530	0.00046	−5298.126070	0.68
(10)	$Hg+BrCl$	−3185.073698	−3185.100943	0.00105	−3185.099893	0
	M10	−3185.075524	−3185.102618	0.00130	−3185.101318	−0.89
	TS10	−3185.016124	−3185.026743	0.00076	−3185.025983	46.38
	$HgCl+Br$	−3185.025853	−3185.040684	0.00068	−3185.040004	37.58
(11)	Cl_2+O_3	−1144.080096	−1144.081251	0.012447	−1144.062127	0
	M11a	−1143.757833	−1144.081251	0.013792	−1143.106807	599.47
	TS11a	−1138.092495	−1143.740679	0.00756	−1143.07876	617.07
	M11b	−1143.755347	−1143.742969	0.00885	−1143.111656	596.43
	TS11b	−1143.735350	−1143.746351	0.007174	−1143.554196	318.73
	$2ClO+O$	−1143.518140	−1143.586352	0.00577	−1143.511662	345.42
(12)	$HCl+O_3$	−684.846852	−684.824488	0.017285	−684.824218	0
	M12a	−684.851329	−684.828450	0.018957	−684.826091	−1.18
	TS12a	−681.374497	−684.829426	0.017944	−684.751727	45.49

Table 1 (continued)

Reaction		MP2 (a.u.)[a]	QCISD (T) (a.u.)	ZPE (a.u.)	E_{tot} (a.u.)	E_{rel} (kcal mol^{-1})
	M12b	−684.843996	−684.855444	0.018178	−684.820815	2.14
	TS12b	−684.831978	−684.840049	0.017978	−684.809619	9.16
	ClO+HO$_2$	−684.784520	−684.822574	0.017151	−684.767806	35.40
(13)	Hg+HCl	−612.986498	−613.020378	0.006966	−612.975757	0
	M13a	−612.985227	−613.003788	0.007492	−612.973050	1.70
	TS13	−612.831120	−612.869258	0.001156	−612.825730	94.14
	M13b	−612.985227	−612.869872	0.007499	−612.973050	1.70
	HgCl+H	−1071.99717	−612.887194	0.000682	−612.861167	71.91
(14)	Hg+Cl	−612.317664	−612.354457	0.000000	−612.374833	0
	TS14	−612.327544	−612.363136	0.000000	−612.325185	31.15
	HgCl	−612.363788	−612.387376	0.000682	−612.360326	9.10
(15)	Hg+Cl$_2$	−1072.042400	−1072.089446	0.001316	−1072.037135	0
	M15a	−1072.043815	−1071.922414	0.001554	−1072.037198	−0.04
	TS15	−1071.893184	−1072.089038	0.000958	−1071.887873	93.66
	HgCl+Cl	−1071.997166	−1072.044169	0.000682	−1071.992289	28.14
(16)	Hg+Cl$_2$	−1072.042400	−1072.089446	0.001316	−1072.037135	0
	M16a	−1072.043815	−1071.922414	0.001554	−1072.037198	4
	TS16	−1071.977731	−1072.014882	0.000820	−1071.972832	40.35
	HgCl$_2$	−1072.133971	−1072.168278	0.002176	−1072.127300	−56.58

[a] 1 a.u.=2625.5 kJ mol^{-1} =627.51 kcal mol^{-1}

process, the distance between the Br atom and O (2) reduces from 0.3013 to 0.1956 nm, while the distance between Cl and O (3) reduces from 0.3563 to 0.2012 nm. At the same time, the corresponding O–O bond extends and finally breaks off.

Reaction (5) is a one-step reaction and there is no M formed. This reaction can take place easily in flue gas [26]. It can be seen from Fig. 5 that the distance between Hg and O (2) is 0.1908 nm, and the distances of O (2)–O (1) and O (1)–O (3) are 0.1753 and 0.1265 nm, respectively.

Reaction (11) and reaction (12) are like reaction (2) and reaction (3), and have two transition states (TS) and two intermediates (M). For reaction (11), the process is Cl$_2$+O$_3$→ M11a→TS11a→M11b→TS11b→2ClO+O. The distances between Cl (2) and O (2), Br (1) and O (3) reduce gradually, while the distances between O (2) and O (1), O (1) and O (3) increase gradually. It can be seen from Fig. 3 that the structural transformation in reaction (12) is basically symmetrical. The distances between Cl and O (3) reduce gradually as: 0.2875 nm→0.1897 nm→0.1857 nm→0.1698 nm, the distance between O (2) and O (1) reduces initially, then increases gradually as: 0.1276 nm→0.1344 nm→0.1533 nm→ 0.1510 nm→0.1455 nm→0.1373 nm.

Energy variations in the reaction processes

The energies of reactants, products, Ms and TSs of the reactions were calculated using the QCISD (T) method and the results are listed in Table 1. E_{tot} is the sum of QCISD (T) energy and ZPE.

E_{rel} is the relative energy. The pre-exponential factors and activation energies are listed in Table 2.

The influences of O$_3$ on reactions of Hg^0 with halogen species

Figure 8 shows the reaction rate constants of Hg^0 with halogen species and O$_3$. Hg^0 converts to Hg^{1+} in the reactions with

Table 2 The reaction kinetic parameters at 298 K

Reaction	A (cm^3 mol^{-1} s^{-1})	Ea (kcal mol^{-1})
(1) Br+O$_3$→BrO+O$_2$	7.56×10^{10}	48.87
(2) HBr+O$_3$→BrO+HO$_2$	1.35×10^{08}	21.20
(3) Br$_2$+O$_3$→2BrO+O	3.37×10^{09}	45.48
(4) BrCl+O$_3$→BrO+ClO+O$_2$	8.39×10^{08}	46.90
(5) Hg+O$_3$→HgO+O$_2$	2.75×10^{12}	30.79
(6) Hg+BrO→HgBr+O	8.69×10^{07}	23.71
(7) Hg+Br→HgBr	5.72×10^{12}	38.30
(8) Hg+HBr→HgBr+H	2.87×10^{13}	80.95
(9) Hg+Br$_2$→HgBr+Br	2.43×10^{09}	17.52
(10) Hg+BrCl→HgCl+Br	2.48×10^{12}	48.94
(11) Cl$_2$+O$_3$→2ClO+O	4.26×10^{10}	617.07
(12) HCl+O$_3$→ClO+HO$_2$	3.35×10^{06}	45.49
(13) Hg+HCl→HgCl+H	8.33×10^{10}	94.14
(14) Hg+Cl→HgCl	2.09×10^{09}	31.16
(15) Hg+Cl$_2$→HgCl+Cl	3.06×10^{11}	93.66
(16) Hg+Cl$_2$→HgCl$_2$	1.48×10^{12}	40.35
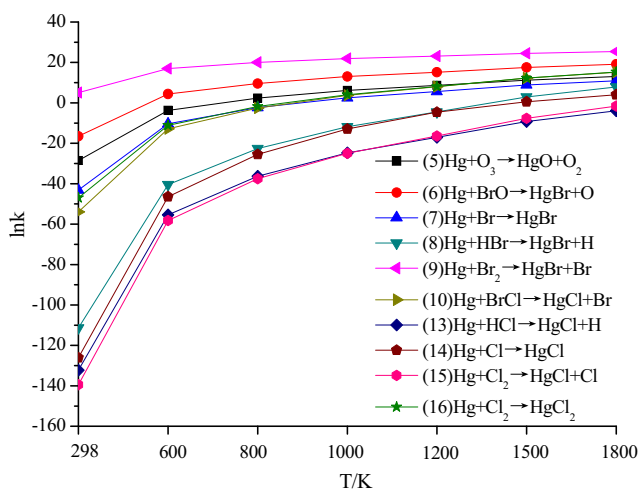
Fig. 8 Rate constants of the reactions of Hg^0 with halogen element and O$_3$

Fig. 10 Comparison of reactions (1), (7) and (14)

halogen species and O$_3$, and halogen species and O$_3$ can be arranged in decreased order as: Br$_2$>BrO>O$_3$>Br>Cl, BrCl>HBr>HCl, Br$_2$>Cl$_2$, according to the reaction rate constants. A distinctive feature is the reaction rate constant of reaction (9) keeps much higher in the whole temperature range than that of all the other reactions. In contrast, reaction (8) and reactions (13)–(15) is hindered by a very high energy barrier and the rate constant is apparently small. In the 573–773 K range, the rate constants of reaction (7), reaction (10) and reaction (16) are almost equivalent.

Figure 9 compares the rate constants of reaction (3), reaction (9), reaction (11), reaction (15) and reaction (16). It is clear that the rate constant of reaction (9) is much higher than that of the other reactions. So, if O$_3$ is present, Br$_2$ and Cl$_2$ will react with O$_3$ and convert initially to BrO and ClO; reaction (3) is inevitably restrained, consequently the oxidation of Hg^0 by Br$_2$ is depressed. Actually, BrO and O$_3$ can also react with Hg^0, the O$_3$ present means Hg^0 is not oxidized by Br$_2$, but by BrO or O$_3$ instead. However, Fig. 9 shows that Hg^0 reacts with Br$_2$ significantly faster than with BrO or O$_3$. Hence, O$_3$ is unfavorable for
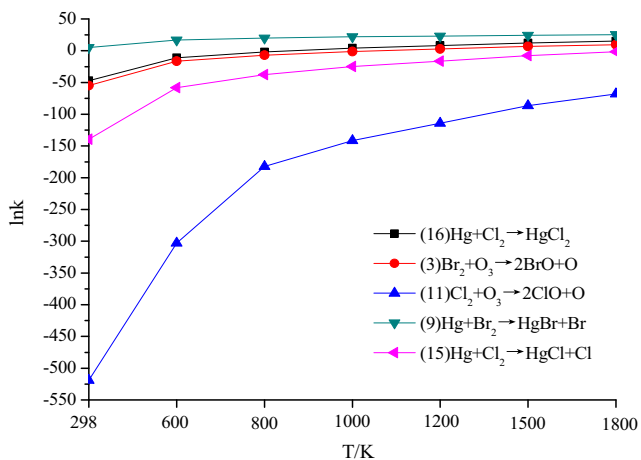
oxidation of Hg^0 by Br$_2$. Hg^0 oxidation in the Hg^0-Br$_2$ system goes much better than in the Hg^0-Br$_2$-O$_3$ system. When reaction (11), (15) and reaction (16), are compared with reaction (3) and reaction (9), the Hg^0 oxidation in the Hg^0-Cl$_2$ system goes much better than in the Hg^0-Cl$_2$-O$_3$ system.

Figure 10 compares the rate constants of reactions (1), (7) and (14), and shows that the rate constant of reaction (7) is just slightly higher than that of reaction (1) and reaction (14), so reaction (7) goes just slightly faster than reaction (1) and reaction (14). Considering only an Hg^0-Br/Cl atom-O$_3$ system, when O$_3$ is not present, Hg^0 reacts with the Br/Cl atom and becomes oxidized. When O$_3$ is present, some of the Br/Cl atoms will react with O$_3$ and convert to BrO/ClO. Although BrO/ClO reacts with Hg^0 faster than the Br/Cl atom, the Hg^0 oxidation by BrO/ClO in the Hg^0-O$_3$-Br/Cl system concerns two reactions, the overall Hg^0 oxidation speed apparently cannot be higher than that of reaction (7). Besides, as the rate constant of reaction (5) is higher than that of reactions (1), (7) and (14), Hg^0 will be oxidized first by O$_3$ but not by the Br/Cl atom.
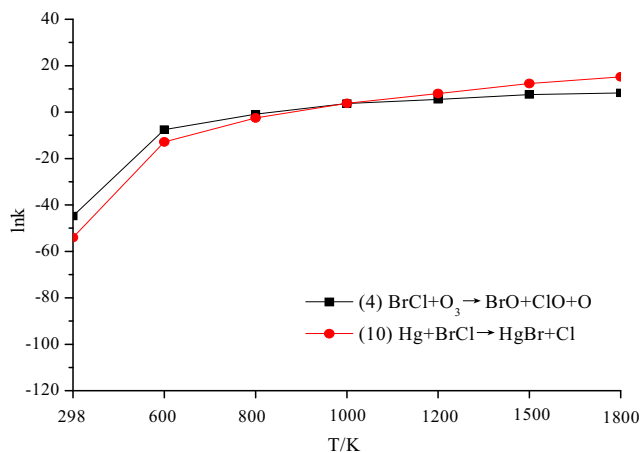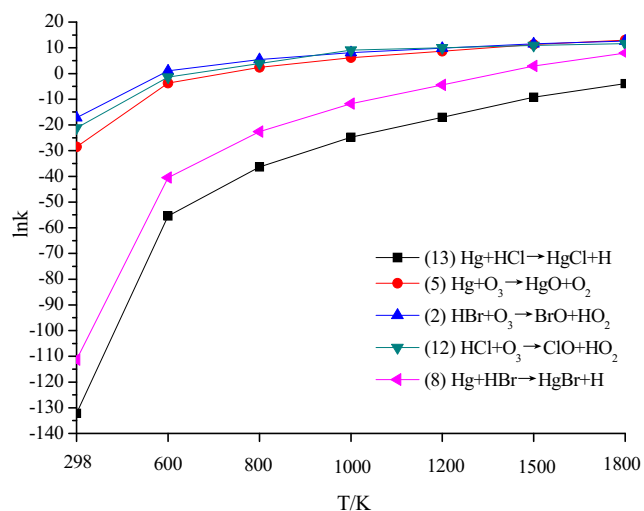

Fig. 9 Comparison of reactions (3), (9), (11), (15) and (16)

Fig. 11 Comparison of reactions (4) and (10)

Fig. 12 Comparison of reactions (*2*), (*5*), (*8*), (*12*) and (*13*)

Figure 11 compares the rate constants of reactions (4) and (10), and indicates that there is no big difference between the rate constants of reactions (4) and (10). Considering that the rate constant of reaction (7) is close to that of reaction (10), the influence of O_3 on Hg^0 oxidation by BrCl is analogous to that of Hg^0 oxidation by the Br atom.

Figure 12 compares the rate constants of reactions (2), (5), (8), (12) and (13). Reaction (13) is hindered by a very high energy barrier and the rate constant is comparatively low. As reaction (2) goes much faster than the other reactions, in conditions where O_3 is present, HBr/HCl prefers to react with O_3 and converts first to BrO/ClO, and Hg^0 oxidation by HBr/ HCl will be replaced by BrO/ClO. Additionally, Fig. 8 shows that BrO reacts with Hg^0 faster than both HBr and O_3; the mixture of HBr and O_3 definitely has better oxidizing Hg^0 capability than HBr or O_3. And the mixture of HBr and O_3 definitely has better oxidizing Hg^0 capability than the mixture of HBr and O_3

Summary and conclusions

Different halogen species and O_3 have different oxidizing Hg^0 capabilities, and all the Br species can react with O_3. As a result, in the Hg^0–halogen species–O_3 system, the conversion of Hg^0 to Hg^{1+} depends greatly on what kind of halogen species is present. For halogen addition technology, bromide or chlorine can be added to coal or injected into the flue gas. At about 1370 K, bromide converts to Br atom and HBr, and the concentrations of the two species are comparable. A temperature decrease then leads to Br atoms recombining into HBr and then Br_2. HBr concentration plateaus at 973 K, Br_2 peaks at 573–773 K. When the temperature is lower than 573 K, the concentration of BrCl increases. Niksa [13] revealed that Hg oxidation begins as the flue gas temperature drops below 873 K, so the influence of O_3 on Hg^0 oxidation

depends on the temperature zone into which the O_3 is injected. At about 1650 K, chlorine converts to Cl atom and HCl. A temperature decrease leads to Cl atoms recombining into HCl and then Cl_2. The HCl concentration plateaus at 993 K, Cl_2 peaks at 583–773 K.

Halogen species and O_3 can be arranged in decreasing order as: $Br_2>BrO>O_3>Br>Cl$, $BrCl>HBr$, $Br_2>Cl_2$ according to oxidizing Hg^0 performance, and Br_2, HBr, Cl_2, HCl and BrCl can react with O_3 and convert to BrO and ClO. The main reactions are as follows: $Br_2+O_3\rightarrow 2BrO+O$, $HBr+O_3\rightarrow BrO+HO_2$, $BrCl+O_3\rightarrow BrO+ClO+O$. thus, O_3 should not be injected into a 573–773 K zone, in which Br_2 and Cl_2 peaks. When the temperature is below 573 K, HBr and HCl are the major halogen species, and there is also some BrCl in the flue gas. As mixture of hydrogen halide and O_3 has better oxidizing Hg^0 capability than hydrogen halide or O_3, and O_3 has better oxidizing Hg^0 capability than BrCl, the presence of O_3 can prominently promote Hg^0 oxidation. Therefore, if halide and O_3 are used simultaneously, O_3 should be used at a temperature lower than the 573 K condition.

It should be mentioned that O_2 ionization in ESP can lead to generation of O_3. The flue gas temperature in ESP is usually about 373 K, and HBr and HCl are the major halogen species in ESP. So, an Hg^0–O_3–HBr or an Hg^0–O_3–HCl system forms in the ESP, which is favorable for Hg^0 oxidation.

References

1. Zhang L, Wong MH (2007) Environmental mercury contamination in China: sources and impacts. Environ Int 33(1):108–121
2. Yudovich YE, Ketris MP (2005) Mercury in coal: review part 2. Coal use and environmental problem. Int J Coal Geol 62(3):135–165
3. Yan NQ, Liu SH, Chang SG, Miller C (2005) Method for the study of gaseous oxidants for the oxidation of mercury gas. Ind Eng Chem Res 44(15):5567–5574
4. Senior CL, Sarofim AF, Zeng T, Helble JJ, Mamani-Paco R (2000) Gas-phase transformations of mercury in coal-fired power plants. Fuel Process Technol 63:197–213
5. Eswaran S, Stenger HG (2008) Effect of halogens on mercury conversion in SCR catalysts. Fuel Process Technol 89:1153–1159
6. Rutter AP, Shakya KM, Lehr R, Schauer JJ, Griffin RJ (2012) Oxidation of gaseous elemental mercury in the presence of secondary organic aerosols. Atmos Environ 59:86–92
7. Lee S-S, Lee J-Y, Keener TC (2009) Mercury oxidation and adsorption characteristics of chemically promoted activated carbon sorbents. Fuel Process Technol 90:1314–1318
8. Agarwal H, Stenger HG (2007) Development of a predictive kinetic model for homogeneous Hg oxidation data. Math Comput Model 45:109–125
9. Tao Y, Zhuo Y, Zhang L, Chen C, Xu X (2010) Impact of flue gas species and temperature on mercury oxidation. Tsinghua Sci Technol 15(4):418–425
10. Goodsite ME, Plane JMC, Skov H (2004) A theoretical study of the oxidation of Hg^0 to $HgBr_2$ in the troposphere. Environ Sci Technol 38:1772–1776

11. Balabanov NB, Peterson KA (2003) Mercury and reactive halogens: the thermochemistry of Hg+{Cl$_2$, Br$_2$, BrCl, ClO, and BrO}. J Phys Chem A 107:7465–7470

12. Tossell JA (2003) Calculation of the energetics for oxidation of gas-phase elemental Hg by Br and BrO. J Phys Chem A 107:7804–7808

13. Niksa S, Naik CV, Berry MS, Monroe L (2009) Interpreting enhanced Hg oxidation with Br addition at plant miller. Fuel Process Technol 90:1372–1377

14. Calvert JG, Lindberg SE (2005) Mechanisms of mercury removal by O$_3$ and OH in the atmosphere. Atmos Environ 39:3355–3367

15. Ye Z, Zygarlicke CJ, Galbreath KC, Thompson JS, Holmes MJ, Pavlish JH (2004) Kinetic transformation of mercury in coal combustion flue gas in a bench-scale entrained- flow reactor. Fuel Process Technol 85:463–472

16. Hongliang G, Jinsong Z, Zhongyang L, Kefa C (2007) Experimental study on hg vapor adsorption of modified activated carbons in simulated flue gas. J Power Eng 27(8):26–30

17. Liu Jing Q, Wenqi ZC (2013) Theoretical studies of mercury-Br species adsorption mechanism on carbonaceous surface. Proc Combust Inst 34:2811–2819

18. Sliger RN, Kramlich JC, Marinov NM (2000) Towards the development of a chemical kinetic model for the homogeneous oxidation of mercury by chlorine species. Fuel Process Technol 65–66:423–438

19. Xu M, Qiao Y, Zheng C, Li L, Liu J (2003) Modeling of homogeneous mercury speciation using detailed chemical kinetics. Combust Flame 132:218

20. Castro L, Dommergue A, Ferrari C, Maron L (2009) A DFT study of the reaction of O$_3$ with Hg^0 or Br. Atmos Environ 43:5708–5711

21. Taylor PH, Mallipeddi R, Yamada T (2005) LP/LIF study of the formation and consumption of mercury (I) chloride: kinetics of mercury chlorination. Chemosphere 61:685–692

22. Shon Z-H, Kim K-H, Kim M-Y, Lee M (2005) Modeling study of reactive gaseous mercury in the urban air. Atmos Environ 39:749–761

23. Subir M, Ariya PA, Dastoor AP (2011) A review of uncertainties in atmospheric modeling of mercury chemistry I. Uncertainties in existing kinetic parameters e fundamental limitations and the importance of heterogeneous chemistry. Atmos Environ 45:5664–5676

24. Xu M, Qiao Y, Liu J, Zheng C (2008) Kinetic calculation and modeling of trace element reactions during combustion. Powder Technol 180(1):157–163

25. Krishnakumar B, Helble JJ (2012) Determination of transition state theory rate constants to describe mercury oxidation in combustion systems mediated by Cl, Cl 2, HCl and HOCl. Fuel Process Technol 94(1):1–9

26. Zheng C, Liu J, Liu Z, Xu M, Liu Y (2005) Kinetic mechanism studies on reaction of mercury and oxidizing species in coal combustion. Fuel 84:1215–1220